Biofilm Matrix Properties in *Pseudomonas aeruginosa* Under Bacteriophage Treatment

A Thesis Presented to the Academic Faculty

By

James Henri Butler

In Partial Fulfillment of the Requirements for the Degree

Bachelor of Science in the School of Biomedical Engineering

Georgia Institute of Technology

December 2020

Biofilm Matrix Properties in *Pseudomonas aeruginosa* Under Bacteriophage Treatment

To Be Approved by

Dr. Jennifer Curtis
School of Physics
Georgia Institute of Technology

Dr. Stephen Diggle
School of Biological Sciences
Georgia Institute of Technology

Dr. Esfandiar Behravesh
School of Biomedical Engineering
Georgia Institute of Technoloy

ACKNOWLEDGEMENTS

Thanks to Dr. Jennifer Curtis for providing advisory guidance and feedback, and to Dr. Stephen Diggle for his feedback and input. I would also like to thank Hemaa Selvakumar for guidance and help with this research.

TABLE OF CONTENTS

	Page
ACKNOWLEDGEMENTS	III
TABLE OF CONTENTS	IV
ABSTRACT	V
Introduction	1
Literature Review	3
Materials & Methods	5
Results	8
Discussion	22
Conclusion & Future Directions	25
REFERENCES	26

ABSTRACT

Biofilms are a specialized structural formation that some bacterial species form when growing in certain environments. One such environment is the human lung, where the bacteria *Pseudomonas aeruginosa* forms biofilms that infect the lungs of cystic fibrosis patients. Techniques used to destroy biofilms have been studied previously, and one promising technique involves the use of bacteriophage. Phage are small, bacteria-targeting viruses that when introduced to biofilms cause the lysis, or destruction of bacterial cells and in some cases, the subsequent destruction of the biofilm. While the impact of phages on biofilms is well known, the changes in physical properties such as extracellular polymeric substance (EPS) distribution and pH distribution in biofilms treated with phage has not been examined in detail. This study seeks to establish pH distribution in *Pseudomonas aeruginosa* biofilms using confocal microscopy and the pH sensitive molecular probe CSNARF4, as well as SYPRO ruby biofilm for the staining of all EPS proteins. Both phage-treated and untreated biofilm samples with the separately added stains of CSNARF4 and SYPRO ruby biofilm matrix were imaged using confocal microscopy and evaluated with a microtiter plate reader, respectively. It was discovered that biofilms treated with phage exhibited little reduction in average pH across all depths into the biofilm, while there was a pronounced increase in protein release into the EPS upon cell death. These results provide greater insight into the effect phages have when being used to treat biofilms and elucidates points of improvement in biofilm treatment.

INTRODUCTION

The spatial organization of microorganisms are typically not found in an ordered manner in most environments. Bacterial cells tend to coalesce into a structure known as a biofilm. Biofilms are organically dense environments in which bacteria can easily prosper, shielded by a matrix which provides protection from intrusion by harmful substances.[1] The matrix surrounding bacteria in a biofilm is composed of extracellular polymeric substances (EPS). The EPS is produced by the bacteria themselves and creates the architectural scaffold that maintains the integrity of the biofilm.[1] Factors that also aggregate into the EPS include extracellular DNA, surfactants, lipids, and nutrients. Recent research in the area of biofilms has generally focused on methods of destruction of biofilms rather than understanding their structural properties.[1,2,3,4] For this reason, research into the dynamics and mechanisms involved in the maintenance of biofilms and the various physical properties they endow will help to better understand how disturbances, such as bacteriophage treatment, change structures within biofilms.

Biofilms in the context of the human body can be found in many forms. The accumulation of dental plaque and the blockage of alveoli in cystic fibrosis for example are both a result of biofilms.[2] Due to the biofilms being especially detrimental to some of the environments they are found in, methods of perturbation to destroy these biofilms have been studied previously. Antibiotics are the most common strategy in clinical applications, however, alternatives are being sought.[5] Bacteriophages (phages), small viral organisms that target bacteria, have been shown to be promising in their ability to perturb biofilms.[6]

The bacterium *Pseudomonas aeruginosa (P. aeruginosa)* is an organism that organizes itself in a biofilm and is one of the common bacteria used in the study of biofilms, due to its role in lung infections and chronic wounds in humans.[5,7,8] It has been shown that under normal conditions *P. aeruginosa* will utilize the biofilm it creates to protect itself from perturbations that activate cell death.[3] The introduction of phage can act to lyse bacteria within biofilms and lead to the destruction of the EPS surrounding the bacteria.[3] Examining this interaction between phage and biofilm can assist to develop mechanistic models that will more effectively guide strategies to minimize biofilm-sustained infections. Changes in the pH during biofilm destruction have previously been shown to increase acidity both within and around the biofilm, resulting in increased resistance to treatments such as antibiotics.[5,8,9,10,11] In this work, we examine the spatial distribution of the pH and EPS throughout *P. aeruginosa* biofilms as pH impacts metabolic processes that sustain bacteria inside the biofilm, and EPS distribution plays a large role in determining the pH internal to the biofilm. Relatively little data exists for these, particularly in the context of phage treatment of biofilms.

This study quantified pH distribution and examined general EPS behavior in *P. aeruginosa* biofilms when exposed to conditions that have been shown to perturb biofilms, with a focus on phage.[6] Examining these properties is of interest to determine effects of phage treatment on biofilm properties involved in the growth and survival of bacterial colonies. Biofilms will be perturbed through the introduction of phages, and will be examined through a

combination of confocal microscopy and spectrophotometric methods to evaluate pH distribution and EPS behavior.[12,13]

LITERATURE REVIEW

This study examined the physical conditions associated with increasing cell death in biofilms due to the addition of phage, specifically pH spatial distribution and changes in the EPS. Gaining a better understanding of how the physical environment of the biofilm changes due to phage exposure may facilitate the effective optimization of the treatment of bacterial biofilms *in vivo*. Biofilm centric infections are able to thrive in environments such as the lungs due to the EPS providing a sub-environment where bacteria can adapt.[1,5] The biofilm's ability to adapt to external conditions more readily makes the study of the extracellular biofilm's structure and chemical properties worthwhile. Mechanisms to disrupt biofilms are the focus on longstanding research efforts[1,4,12] with the practical purpose of assisting in prevention or removal of bacterial infections in diseases such as cystic fibrosis.[14] As a result, much research has previously been focused on identifying these strategies and testing strictly for their efficacy in removal of these bacterial communities. Modeling and characterization of physical parameters within biofilms has only recently become a subject of interest in biofilm research, and in the context of phage treatment, little experimental work has been reported thus far.[4,7] Thus, study of the EPS structure and physiochemical properties (e.g. pH) of biofilms during perturbation can lead to a better understanding of mechanisms leading to destruction.[1]

Biofilms are predominantly unaffected by many techniques used to normally deal with bacterial infections such as antibiotics, ultraviolet radiation and immune defense due to their complex extracellular matrix (EPS) comprised of many different substances.[1] Phage therapy, the use of bacteriophages to disrupt the structural integrity of the bacterial colony, has previously shown potential in the treatment of biofilms.[4] Phages have been shown to be an effective antimicrobial agent in the context of in vitro human lung models.[7] The importance of pH to biofilm function is that bacterial metabolic processes depend heavily on pH, which can be altered when cell lysis is induced by phages.

The use of confocal microscopy to analyze spatial properties of biofilms is a central technique in many studies.[13] Confocal microscopy involves using various light wavelengths to excite fluorescent dyes in a sample, which will subsequently fluoresce at another longer wavelength that can be captured and imaged. A recent review compiled by Schlafer & Meyer confirms that confocal microscopy is extremely useful due to the ability to fluorescently stain nearly every component relevant to the study of the EPS and to be able to precisely quantify various properties of the biofilm.[13] Prior to the widespread use of bacteria genetically modified to fluoresce under certain light wavelengths, fluorescently-labeled lectins were used due to their enhanced imaging resolution caused by a tightly regulated fluorescent intensity.[15,16] Fluorescently-labeled lectins are fluorescently-labeled proteins that bind to specific molecular targets, and are useful for analyzing samples that are isolated from in vivo environments.

Previous studies examining pH in biofilms have used CSNARF4, a pH-sensitive ratiometric fluorescent probe.[9] The ratiometric approach to imaging requires obtaining the emission intensity of the dye at two different wavelengths for a given location. These two

intensities can then be related using a function seen in equation 1 to obtain an output pH for the given location. R is the ratio of intensities for the different wavelengths, defined as $F_{\lambda 1}/F_{\lambda 2}$. $F_{b(\lambda 2)}$ and $F_{a(\lambda 2)}$ are the limiting fluorescent intensities of the second wavelength from the titration performed to calibrate the dye. Similarly, R_a and R_b are the limiting values of the ratios from the calibration, defined as $R_x = F_{x(\lambda 1)}/F_{x(\lambda 2)}$ for $x = \{a, b\}$. The pK_a of the dye is given found through calibration of the dye, the procedure for which is discussed in the methods section.

Eqn. 1) $$pH = pK_a - \log\left[\frac{R-R_b}{R_a-R} \times \frac{F_{b(\lambda 2)}}{F_{a(\lambda 2)}}\right]$$

Initial studies examining the relationship between pH and biofilms have focused on examining pH in microenvironments in the biofilm and assessing the use of CSNARF4 in determining pH.[9] It was found that typical pH ranges with a biofilm are between 5.6 and 7.0 where little to no cell death occurs, with the average pH being 6.7±0.1.[9] It has been noted that more acidic environments in *P. aeruginosa*, pH's of 6.4 and lower, lead to significantly enhanced resistance to bactericidal effects.[11] Acidic environments caused by biofilms have also been examined in extreme pH ranges in dental biofilms, where the cause pH ranges lower than 4 have been attributed to biofilm formation.[17] Monitoring lower pH ranges shows the main downside to using CSNARF4, in that CSNARF4 will not give correct pH information when exposed to pH's lower than 5.5, as demonstrated by Schlafer *et al*.[18] This however can be solved using a different excitation and emission frequency approach validated by Burdikova *et al*.[10] The ability to monitor a lower pH range is needed if pH changes caused by phages lysis cells cause a pH drop below the 5.5, however there is a lack of previous literature relating to examining the cause of drops in pH as biofilms are treated.

Past studies involving evaluation of the EPS have looked at composition and structural properties by using fluorescent stains. [6,17,18,19] Different EPS stains have targeted a variety of components, including proteins, extracellular DNA, lipids, and polysaccharides.[6] Previous studies involving the use of these stains have done so under culture conditions different from those that will be used in this study, such as flow-cells and cryo-mold sectioning.[13,19,20,21] Static biofilm growth-environments that still allow for change over time have not yet been examined using stains. It is expected that in a static growth-environment there will be enhanced production of EPS, particularly increased protein production dependent on cell lysis, and subsequent decrease of polysaccharide production. In terms of culture times for biofilm growth to ensure EPS is present in the matrix, previous studies using *P. aeruginosa* have used culture times as low as 2 hours[3] and as high as 36 hours.[7]

METHODS & MATERIALS

Strain and Culture Conditions

For optimizing microscopy visualization of the biofilms, *P. aeruginosa* NPAO1 containing a GFP plasmid was used. Once biofilm growth was optimized, the wild type (WT) *P. aeruginosa* NPAO1 was used to enable visualization of the pH throughout the biofilm. WT NPAO1 and GFP strains were streaked onto LB agar plates and incubated until colonies formed. All incubation was carried out at 37°C unless otherwise stated. The strains were then cultured in LB broth overnight, then moved to a subculture of LB broth, cultured for 4 hours then diluted to an OD of 0.0125. Samples were then prepared in a 96-well glass-bottom plate at 250 µL of subculture per well and incubated 24 hours to grow the biofilm before addition of dye. The *P. aeruginosa* PEV2 phage was used for phage treatment.

For use in spectrophotometry of the EPS, WT NPAO1 was streaked on a plate, cultured overnight and then moved to a subculture. Subsequently, the subculture was diluted to the necessary concentrations in the range of 0-10^9 cfu/ml before being added to a plastic 96-well plate in appropriate volumes together with the relevant fluorescent dyes (described below). Each well volume totaled to 254 µL after all constituents had been added. Biofilms used for spectrophotometry were then incubated for 4 hours before the addition of phage, different to the incubation period for pH experiments.

Dye Calibration

The C-SNARF-4 (Thermofisher Scientific) fluorescent ratiometric probe was used to quantify pH in solution. C-SNARF-4 was prepared from a 1 mM stock solution diluted in DMSO. Calibration of the dye and the creation of titration curves necessary for ratiometric analysis, converting fluorescence emission ratios to pH, was carried out as outlined by Hunter *et al.* [11] Buffers for pH's ranging from 5.4 to 7.4 in increments of 0.4 were prepared as 0.1 M solutions of sodium phosphate dibasic and citric acid (for pH's 5.4 and 5.8) and sodium phosphate dibasic and sodium phosphate monobasic (for all other pH's). 250 µL of each solution was added to individual wells in a 96-well glass-bottom plate, and CSNARF4 dye was added at 10 µM to each well. Images were then taken in accordance with the image collection protocol outlined in the image collection section. All samples were prepared in duplicate for calibration. After images were collected, the pH titration curve values were found by taking the pixel intensities corresponding to the 580 and 640 nm channels utilizing the known values of the pH, limiting curve values, and fluorescent intensity in equation 1 to calculate the pKa of the dye. A nonlinear-curve fit was then performed on the titration curves to evaluate performance between known and predicted values.

pH Sample Preparation

Samples without any phage added were used as the control group. PEV2 phage at concentration of 10^11 pfu/mL in LB broth was added to the appropriate samples at 20 µL each

after having incubated for 12 hours. The CSNARF4 dye was added to samples at 10 µM concentration after a total of 24 hrs total culture timeframe (12 hrs biofilm growth + 12 hrs phage exposure) and allowed to equilibrate while incubating for 15 minutes prior to collecting images.

EPS Spectrophotometry Sample Preparation

Preliminary evaluations of SYPRO ruby biofilm matrix (Invitrogen), calcofluor (Thermofisher), SYTO-9 (Thermofisher) and propidium iodide (Thermofisher) were done. SYPRO ruby matrix stains proteins, calcofluor stains chitin and polysaccharide chains. SYTO-9 and propidium iodide are used for live and dead cell staining respectively. All dyes were added at the time of seeding for each biofilm culture, Ruby matrix and calcofluor additionally were put into other cultures at the time of phage addition during initial screenings. In all cases, 10 µL of dye diluted in LB was added to each well, and 14 uL of phage diluted in the range of 0-10^9 pfu/mL. Biofilms used in spectrophotometry experiments were incubated for 4 hours before the addition of phage. After the initial screening, it was determined the range of 0-10^4 pfu/mL for final phage concentration and 10^7-10^9 cfu/mL for final bacterial concentrations were of interest when studying phage effects on EPS. Due to overlapping emission spectra, stain combinations were evaluated for ruby matrix plus calcofluor, and SYTO-9 plus propidium iodide. All final concentrations of stains were made to be as recommended by the manufacturer, apart from ruby matrix which was added at 10 µL of the 1X concentration directly to the well.

EPS Spectrophotometry Collection

A plate reader was used to extract information on OD, as well reading intensities using the excitation and emission spectra peaks for each fluorescent stain, as recommended by the respective manufacturers, then adjusted to avoid signal overflow on the reader. Format: excitation (ex)/emission (em). SYPRO ruby biofilm matrix: 450/610; Calcofluor: 355/400; SYTO-9: 486/550; Propidium Iodide: 535/617. For initial screening, the plate was read once at all ex/em spectra for each well without phage addition. Initial kinematic studies on just ruby matrix in the phage-treated biofilm samples were performed over 16 hours, then 4 hours in subsequent experiments, collecting intensity information every 30 and 15 minutes, respectively.

For the initial screening experiment, bacterial concentrations of 0, 10^6, and 10^9 cfu/mL were used with each dye or combination of dyes as outlined and shown in results. For the secondary screening, phage concentrations ranged from 10^1 to 10^9 pfu/mL with a control of 0 pfu/mL, and bacterial concentrations ranging from 10^1 to 10^9 cfu/mL with a control of 0 cfu/mL. Both phage and bacterial sample concentrations were increased by a factor of 10 for each sample. Secondary screening had a total of 90 samples with unique combination of each phage and bacteria concentration. This experiment had signal reads taken every 30 minutes for 16 hours. The third experiment used bacteria concentrations in the range of 10^7 to 10^9 cfu/mL, and

phage concentrations from 10^1 to 10^4 pfu/mL with 0 pfu/mL control, all samples done in triplicate. Reads were taken every 15 minutes for 4 hours. More detail is shown in the results section.

Image Collection

All biofilm images were taken on a confocal laser scanning microscope equipped with a 40x/1.00 NA oil immersion objective lens, a 488-nm laser, and dichroic beam splitters with ex/em of 488/720 and 488/560 nm. A 40x/1.00 NA oil immersion lens was used to collect 1024x1024 resolution images in the horizontal plane of the sample with a zoom factor of two. Samples with CSNARF4 dye were excited at 488 nm, and dye emission was detected in two channels at 580 and 640 nm. Samples with ruby matrix were excited at 488 nm, and emission detected at 640 nm. Image stacks were taken by manually adjusting the scope to the bottom of the biofilm, and imaging from 5 µm below the biofilm to 40 µm above the bottom in increments of 0.2 µm. Stacks were taken at the center of the sample, one per sample. The control groups for these experiments were the biofilm samples of the WT NPAO1 strain without phage added, the group treated with phage was still the WT NPAO1 strain of *Pseudomonas aeruginosa*.

Image Analysis

Images were analyzed using MATLAB, acquiring average pH values as a function of height of the image stack, utilizing the ratiometric procedure mentioned previously to compute pH as a function of the ratio between fluorescence in the two emission channels monitored by the microscope. Using ImageJ, the local pH was extracted by finding the average pH for 50 μm^2 areas, corresponding to roughly 100 by 100 pixels in the 1024x1024 image. The pH distribution mean and standard deviation was then calculated at each incremented vertical height within each are of interest in the image stack of the biofilm for each group. Test for significant change in pH on treatment of phage was done by performing a t-test on the means of the pH value at the equivalent height in each stack, with respect to control. The p-values obtained as a function of height were then used to determine which sections of the biofilm had a significant difference in pH when treated with phage.

RESULTS

pH Calibration

To determine the pH within the biofilm using the CSNARF4 dye, a calibration curve of fluorescent intensities with respect to pH of different buffers was obtained. Generation of the curve involved the use of two models. The first model takes a simple ratio of the two fluorescent emissions, then correlates this number to the pH using an exponential fit. This was used previously by Hunter *et al* for the creation of a single curve.[9] The second model uses two nonlinear curves fitted to the emission intensities of the 580 and 640 nm emission wavelengths. The predicted pH's are retrieved individually for 580 and 640 nm curves, the average is then taken to obtain the final predicted pH. The data obtained from this buffer analysis was tested against the simple ratio model, then against the two-curve approach. The simple ratio saw lower performance than the two-curve approach, the fit yielding an r-squared value of 0.7683 while the fit for the averaging curve yielded an r-square value of 0.86. It is important to note these r-squared values correlate the predicted pH of each model to the actual pH in buffers used, not of the fit curves themselves. Due to the higher performance of the averaging curves, this model, Figure 1, was used for analysis and more accurate prediction of pH values in the actual biofilm samples. Two different fits were tested against the buffer data set, fit 1 being a negative-quadratic and fit 2 being an inverse hill function. Both were used *ad hoc* to fit the trend of the buffers. Fit 1 suffers from bad performance in the range pH range of 5.5 to 6, while fit 2 does not perform well above pH's of 6.5. Both fits perform badly in the near-neutral pH range. As the expected pH range in the biofilm was 6.7 and below, fit 2 was chosen for use.

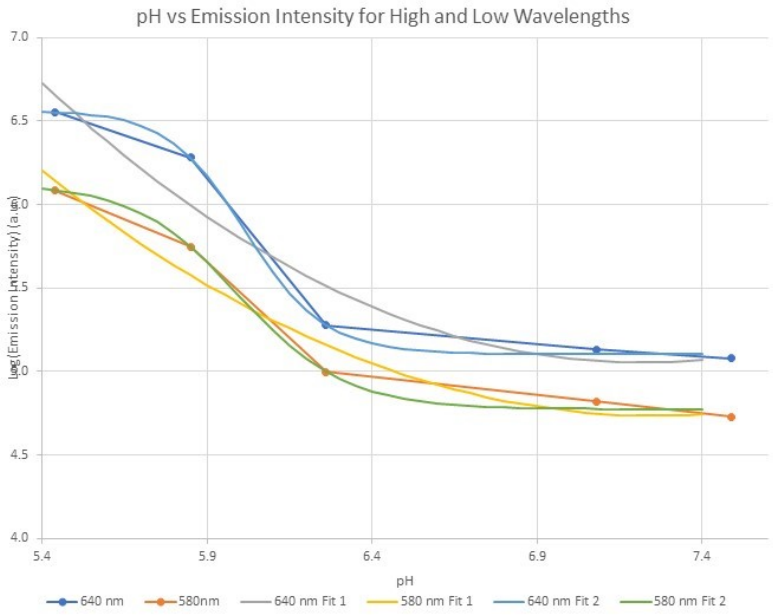

Figure 1: Two Curve Model; Titration curves relating pH to higher and lower emissions. Linear pH scaling fitted to a negative-quadratic nonlinear curve in fit 1, and an inverse hill function in fit 2.

pH distribution in phage-treated *P. aeruginosa* biofilms

Analysis of pH in phage treated biofilms was performed to determine if significant changes in pH occur due to phage treatment, focusing predominantly pH changes in the biofilm as a function of depth. Biofilms for pH analysis were grown for 12 hours before adding phage. The samples were then incubated for another 12 hours before the addition of CSNARF4 dye. The samples with dye added were then incubated for another 15 minutes before imaging. WT NPAO1 was used for images as GFP-tagged NPAO1 has significant overlap of spectrum with the dye, and therefore the GFP strain was not used alongside CSNARF4.

150 Slices were imaged from 0 to 30 µm from the bottom of the biofilm. Visual inspection of the images at various slices revealed the dye did not aggregate within certain areas of the biofilm. These structures where the dye failed to penetrate have similar shapes to densely localized colonies of bacteria that form within biofilms, which can be seen in Figure 2 in the areas where there is an absence of emission intensity in both the wavelengths. Due to noise in these areas, the resulting ratiometric combinations still yield pH values that cannot be verified properly using the calibration curves. These areas were therefore excluded from pH analysis when they appeared.

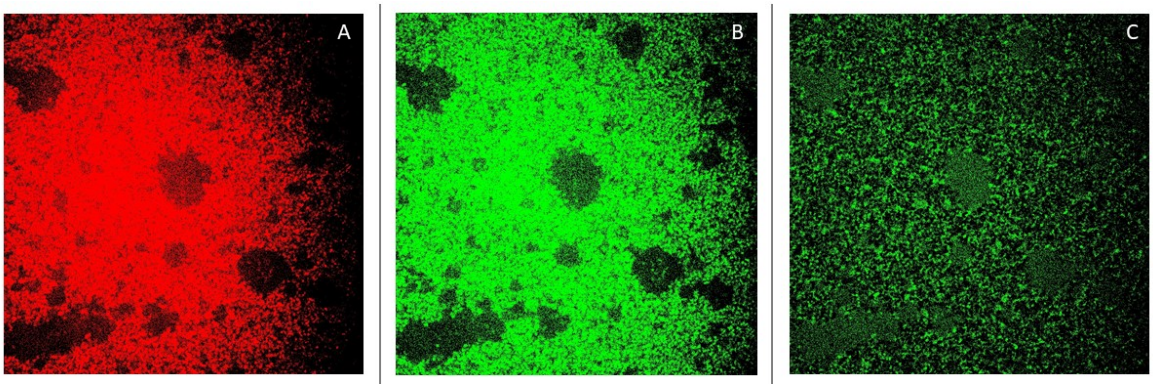

Figure 2: Fluorescent Emission of CSNARF4 in WT NPAO1 without phage. Sample excited at 488 nm, image (A) is intensity at 640 nm emission, image (B) is intensity at 580 nm emission. Image (C) is the resulting ratiometric combination of (A) and (B). Images here adjusted for visualization purpose. Higher intensities correspond to higher pH values in image (C), in the range of 5.6 to 7.6. In (A) and (B), areas that can be seen to have little emission appear in the combined image as noisy areas, these are excluded from analysis.

Certain dense areas within the biofilm had little to no signal at the wavelengths used. Previous literature suggests that when the dye penetrates into single bacteria, it will fluoresce at a higher intensity causing the pH to appear higher than in reality when using a simple ratio approach.[9] However, it is observed here that dense bacterial colonies do not emit high signals. The ratiometric approach used here does yield a similar conclusion to previous literature in that permeation gives a higher pH, though this is due to both images having low signal to noise ratio in those areas. It is possible that dye does permeate these bacterial clusters, but chemical processes that occur within those clusters may cause the dye to fluoresce at different wavelengths than what is monitored here or become inactive otherwise. Further work outside

of this study should be performed to determine whether this effect manifests physically or is just observed for other reasons. If the dye is physically unable to penetrate into bacteria located in these clusters, this may elucidate other properties relating to biofilm resisting other treatment mechanisms.

Selection of areas of interest to analyze were taken at 9 different points in the biofilm for each of the 5 samples, throughout the entire image stack. An area of interest corresponded to a 100x100 pixel (px) square in the x-y plane of a given image stack (where one x-y image corresponds to 1024x1024 px total), for all height values in that stack (stack size of 0 to 30 μm, or 150 200nm slices). pH values for each area of interest versus height were obtained using the fits acquired as discussed previously. One such example of a single comparison between a point in a normal biofilm versus a phage-treated biofilm is shown in Figure 3a. This region was selected based on the similarity between the two areas in the treated and untreated samples. The similarities were seen in terms of distance between dense bacterial communities. Height variation was the focus of the remaining analysis, as pH variation across a single x-y slice was found to be very small (<0.1 maximum). For analysis regarding the pH of larger areas, 9 areas of interest in each biofilm xy plane were selected at random (100x100 px). All areas were verified to have no overlap with a dense bacterial community or each other. If any of the randomly selected areas was found to have overlap, then the area was discarded, and a new random point was selected until the criteria was met.

Once all areas had been selected, the average pH of all areas for a given height in biofilm was calculated. This average was taken at the same relative height into the biofilm for all phage-treated and untreated samples. This was then performed for all heights in all samples, seen in Figure 3b. A t-test was then conducted on the pH at all equivalent heights in the biofilm. It was observed that the pH for both treated and untreated samples did not show a large magnitude in difference (<0.01 pH). A one-way ANOVA was conducted on the final 2.6 μm of the pH averages, revealing that there was no significant difference of any neighboring pH between the phage treated and untreated groups at the bottom of the biofilm. The pH difference for Figure 3a appears as much larger than the averaged pH's shown in Figure 3b. This is most likely due to the random nature of the 9-point selection across all 5 samples, and the fact that biofilms did not have large variations in pH in a single sample. The random selection did not bias towards areas of similar bacterial density as it was not possible to do so, this may have led to a smaller standard deviation when considering the large sample size of these points, n = 45.

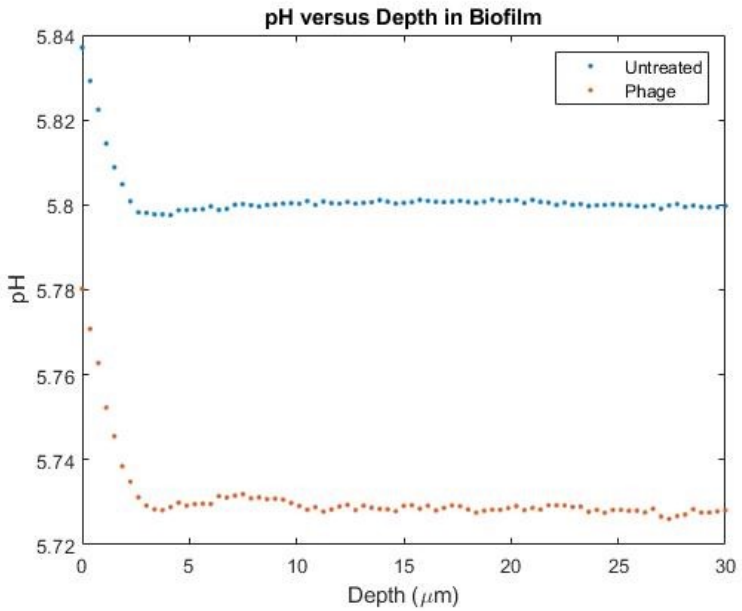

Figure 3a: pH of a single area of interest analyzed in biofilms cultured for 6 hours. Horizontal axis represents depth into the biofilm with respect to the bottom of the biofilm. Vertical axis is the pH average in the area of interest.

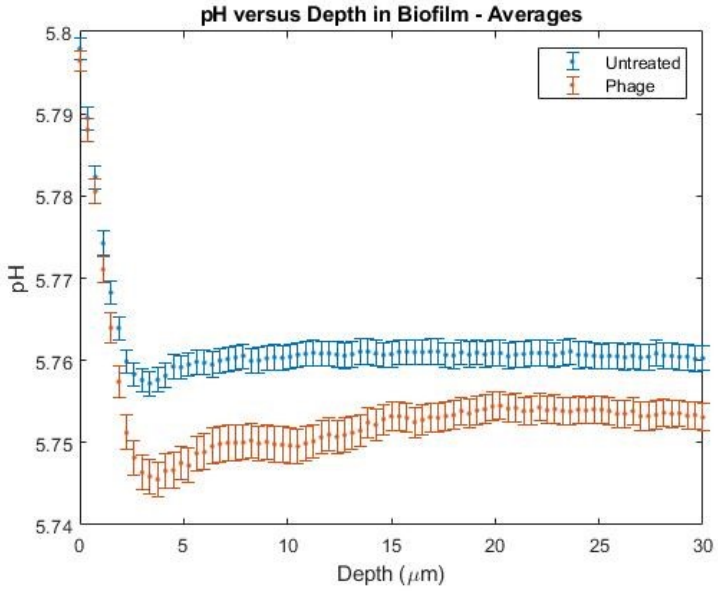

Figure 3b: Average pH across 9 areas of interest in each biofilm sample. Error bars represent one standard deviation. T-test was conducted on pH at each depth in the stack. All points had a significantly lower pH in the phage-treated sample compared to the untreated, at alpha < 0.001. An ANOVA computed on the final 2.6 µm of sample depth showed no significant difference in the pH.

EPS Evaluation

Multiple fluorescent EPS stains were evaluated to determine and validate the best dyes for measurement via spectrophotometry to understand the effect of phage treatment on EPS changes within the biofilm. Further, we examined whether it is possible to use multiple stains simultaneously. Different emission wavelengths were tried for certain stains due to poor signal or saturation, as well as attempting to avoid spectrum overlap. Table 1 shows the stains used, stain targets, and excitation and emission (ex/em) wavelengths corresponding to each stain. Emission wavelengths consist of expected wavelengths as prescribed by the manufacturer; actual wavelengths consist of those that were used after optimization. This was needed to ensure that the stain fluorescent behavior is as expected, or can be corrected for depending on any chemical differences between culture conditions used in previous studies. Each sample was seeded with bacteria and the relevant EPS stain before being incubated for 4 hours before being read on the spectrophotometer. The results are summarized in Figure 4a.

Table 1: Stains evaluated and corresponding excitation/emission wavelengths

Stain	**Target**	**Excitation Wavelength (nm)**	**Expected Emission Wavelengths (nm)**	**Actual Emission Wavelengths (nm)**
Calcofluor White	Chitin, Polysaccharides	355	433	500
SYPRO Ruby Biofilm Matrix	Proteins	450	610	610
SYTO-9	Live Cells	486	501	550
Propidium Iodide	Dead Cells	535	617	617

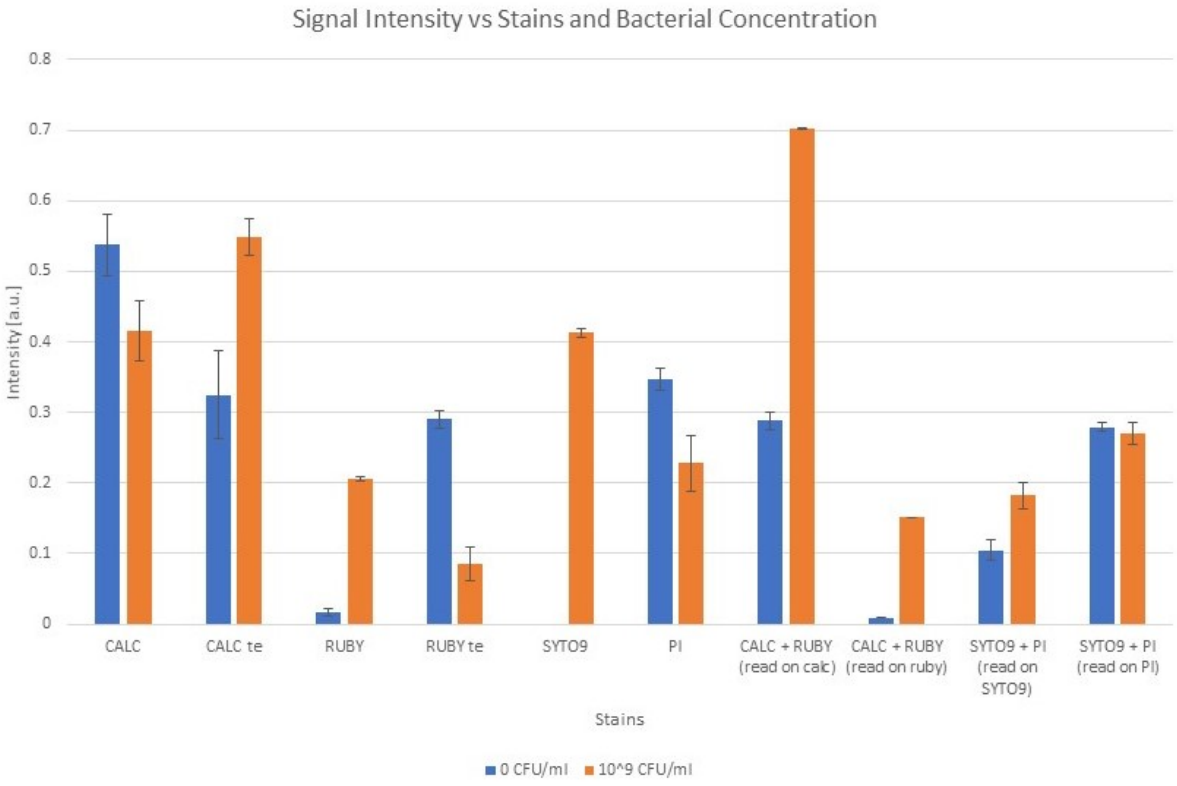

Figure 4a: Main results of stain screening. Signal Intensity Graphs represent signal read from each stain on its' own excitation and emission, except in samples where stains were combined. All values normalized to an arbitrary high intensity reading of 10^4 for visualization purpose (i.e. all readings were divided by 10^4, an original intensity of $5x10^3$ appears as 0.5). 'te' denotes samples where stains were added 30 minutes prior to reading intensities rather than at time of sample seeding. 0 cfu/mL represents a control where no bacteria were present.

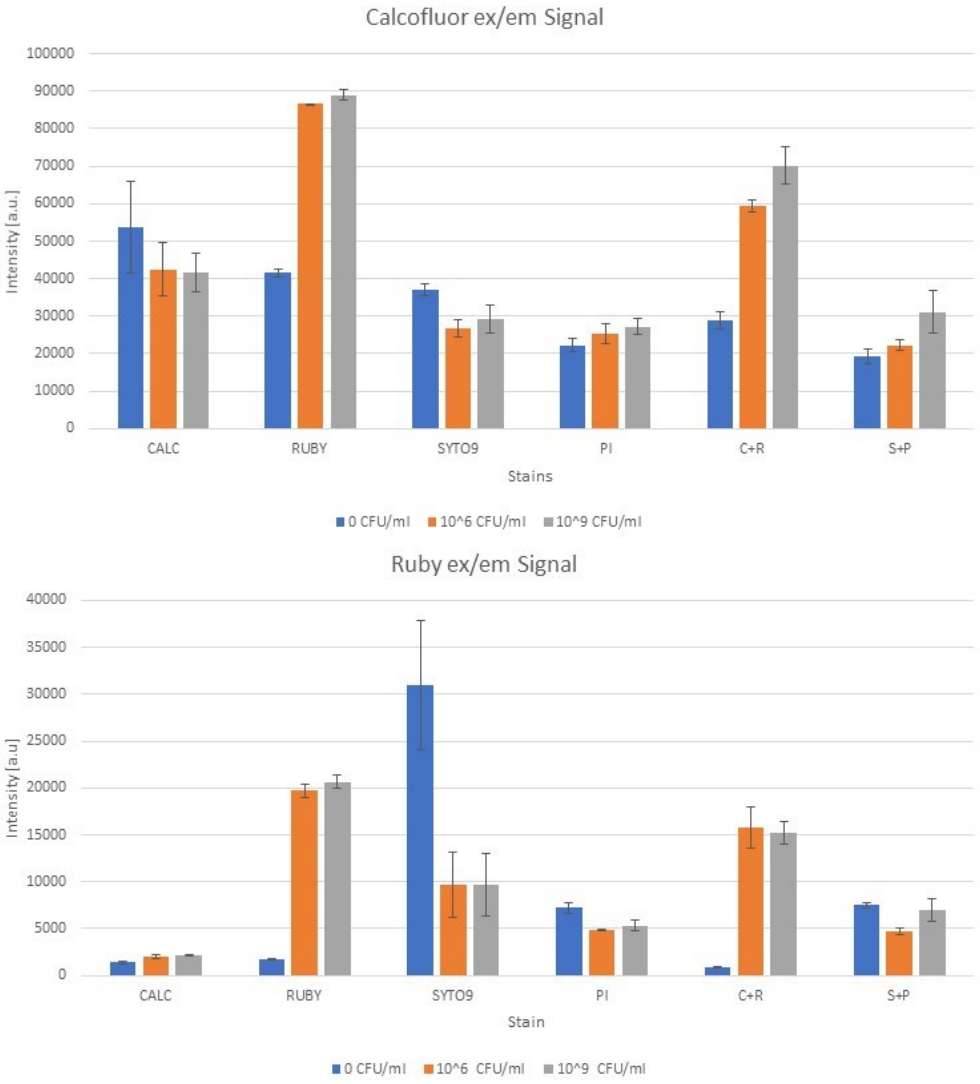

Figure 4b: Ruby and Calcofluor Signals. Shows signal received from each sample regardless of dye used. e.g. Calcofluor ex/em Signal shows the signal received using the calcofluor (CALC) excitation and emission wavelengths for the samples containing only calcofluor (CALC), only ruby (RUBY), only SYTO9, only propidium iodide (PI), and the combinations of calcofluor with ruby (C+R) and SYTO-9 with propidium iodide (S+P). Calcofluor ex/em: 433/500nm, Ruby ex/em: 450/610nm.

Two outcomes that informed the future experiments were taken from this initial stain screening. First, stains added at the time of seeding performed better on average than stains added 30 minutes before taking readings. This can be seen in Figure 4a. Stains were added to samples at the same time as bacterial seeding to grow the biofilm, equilibrating with the biofilm during growth for a total of 4 hours. This is different of those samples marked with “te”, these samples did not have EPS stains added until 30 minutes prior to reading with the spectrophotometer. Signals for stains that were added at the time of bacteria seeding are higher in intensity than those added 30 minutes prior to reading for 10^9 cfu/mL samples. The

opposite is true for 0 cfu/mL samples, where unbound stains that have not been given long to equilibrate into the solution fluoresce at a much higher intensity. To avoid this unbound fluorescence issue, and to give better signal in bacterial samples, EPS stains were added at the time of bacteria seeding for all later experiments.

Second, utilizing combinations of stains is not viable, as shown in Figure 4b. Figure 4b shows signal intensity for a given stain's excitation and emission wavelengths. For example, the "Calcofluor ex/em Signal" graph was obtained by using the excitation and emission wavelengths of 433 and 500 nm for every sample that was read during the experiment, regardless of whether the sample contained calcofluor. Based on optimizations performed to acquire signal, ruby matrix and propidium iodide share overlapping spectra, and therefore cannot be combined, calcofluor and SYTO-9 share the same issue. When looking at the signal intensities obtained from this experiment, it appears ruby matrix overlaps heavily with unbound SYTO-9 stains, and therefore cannot be used in combination, unfortunate due to the fact that imaging live cells and proteins in the EPS would be good for localization. Additionally, calcofluor cannot be used alongside ruby, as the ex/em gives higher signal from ruby than calcofluor itself. As ruby matrix had highest performance all around and was most applicable to staining the EPS, more so than calcofluor, ruby matrix was used for subsequent experiments. A point of note is that ruby matrix gives higher signal when using the excitation and emission wavelengths intended for calcofluor. Calcofluor wavelengths were not used in subsequent experiments with ruby matrix to avoid possible signal saturation. Additionally, the signal emitted by ruby using its respective excitation and emission wavelengths was not exceedingly low with respect to the control. Regardless, this phenomenon illustrates the need for stain screening, as the spectra that gave optimal signal were not as expected from literature.

The purpose of the next experiment was to screen the entire range of applicable bacterial concentrations and phage concentrations to examine which conditions would be viable for thorough examination. A total of 90 samples were evaluated at varying bacterial and phage concentrations (N=1 for each sample condition). All bacterial concentrations were incubated for 4 hours with ruby matrix allowing for biofilm growth before the addition of phages. Each sample had a different bacterial and phage concentration ranging from 10^1-10^9 cfu and pfu per mL (incrementing by a factor of 10), as well as a control which contained no added phage. It was found that changes over the 16-hour experiment in OD and ruby signal occurred in samples with both bacterial concentration ranges of 10^7 to 10^9 cfu/mL and phage concentration ranges of 10^1 to 10^5 pfu/mL. A sample of what the data looks like for a single starting bacterial concentration (10^9 cfu/mL) and all nine pfu concentrations is shown in Figure 5.

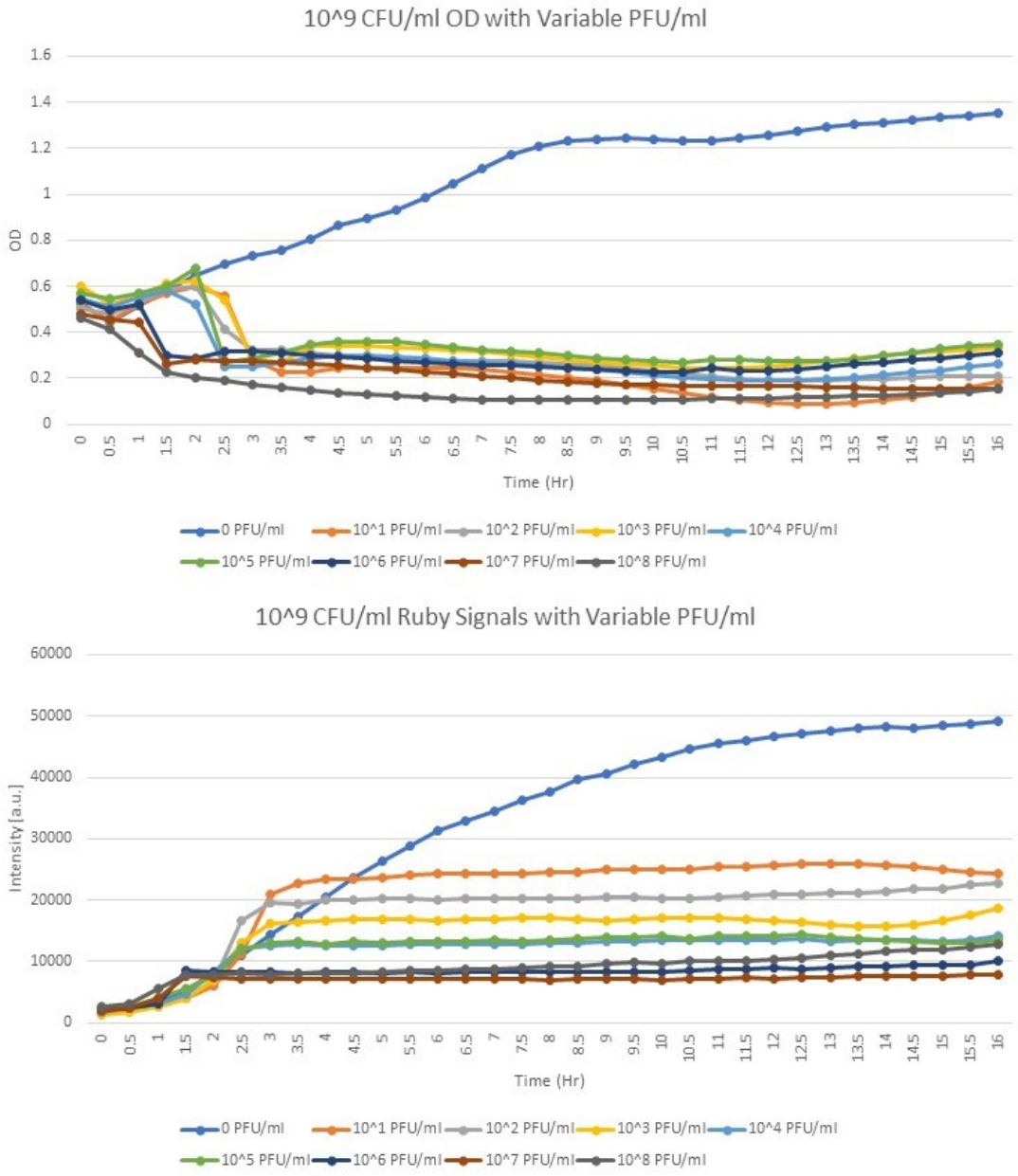

Figure 5: Bacteria and phage concentration screening. This shows the OD and ruby signal of the 10^9 cfu/mL bacterial concentrations against varying phage concentrations. Control is 0 pfu/ mL.

From the result of this second series of experiment, it can be seen that EPS production ceases once enough bacteria have been destroyed by phages, following a similar growth curve to the control until the point of plateauing, which occurs before 4 hours of phage activity, plateauing more quickly with increased phage concentration. The ruby intensity and OD plateaus occur at the same time points for each respective phage concentration condition. Interestingly, it appears all phage conditions end around a similar OD of 0.2. This plateauing OD compared to the initial OD for that sample is a fraction of 42.0% ± 9.5% of the original OD. However, if the OD remains constant while bacteria continue to grow, it would be expected

that the ruby intensity should then increase as more proteins from bacteria are released from the dead cells through lysis. This may be explained as the point where the number of phages and bacteria reach a saturated point where phages have destroyed all live cells, leaving only the detritus of lysed bacteria to contribute toward the OD. Further work would be necessary to evaluate this hypothesis, specifically by targeting live cells as targets to quantify during this interaction.

The plateauing behavior after a brief overshoot of the control intensities gives preliminary indication that bacterial lysis, and the destruction of bacteria cell walls leads to much higher levels of proteins in the EPS. To prove this fully, an imaging experiment would need to be performed. The plateauing behavior of the OD and ruby intensity is dependent on phage concentration, as samples with higher phage concentrations experience plateauing earlier than lower phage concentrations. Ruby intensity corresponding to proteins in the EPS overshoots control intensity for every phage condition, with higher phage concentrations experiencing a lower magnitude of an overshoot, explained by less bacteria being in the biofilm at the timepoints at which they occur. Thus, the phage to bacteria ratio appears to determine how quickly protein production in the EPS stops. This informed the final experiment using spectrophotometry by only having to examine the first 4 hours of the phage-biofilm interaction at the operable ranges as described previously.

The next experimental investigation will reveal why more data at the different cfu values from the 90 assays performed here has not been examined closely at this point. In retrospect, we will unfortunately demonstrate that the use of the ruby at lower cfu concentrations is incompatible with the analysis we are trying to achieve, and the results at values other than 10^9 cfu/ml cannot be used.

The last experiment involving spectrophotometry examined the narrowed-down concentration ranges more precisely over the initial 4-hour period during which the EPS appears to actively change as phages continue to operate within the biofilm. From the previous assay, it was identified that the ranges where EPS change occurs corresponds to the 10^7-10^9 cfu/mL and 10^1-10^4 pfu/mL concentrations for bacteria and phage, respectively. Samples were prepared in triplicate, with one condition for each combination of bacteria and phage concentration, as well as control with no phage. Fifteen different conditions were examined totaling 45 samples. Figure 6 summarizes the results for the 10^9 cfu/mL bacterial concentration. Figure 7 uncovers a key issue with use of ruby matrix that impacts analysis of bacterial samples with cfu/ml less than 10^9. As discussion below will explain, this result represents the reason why more data from the expansive parameter study was not shared in above.

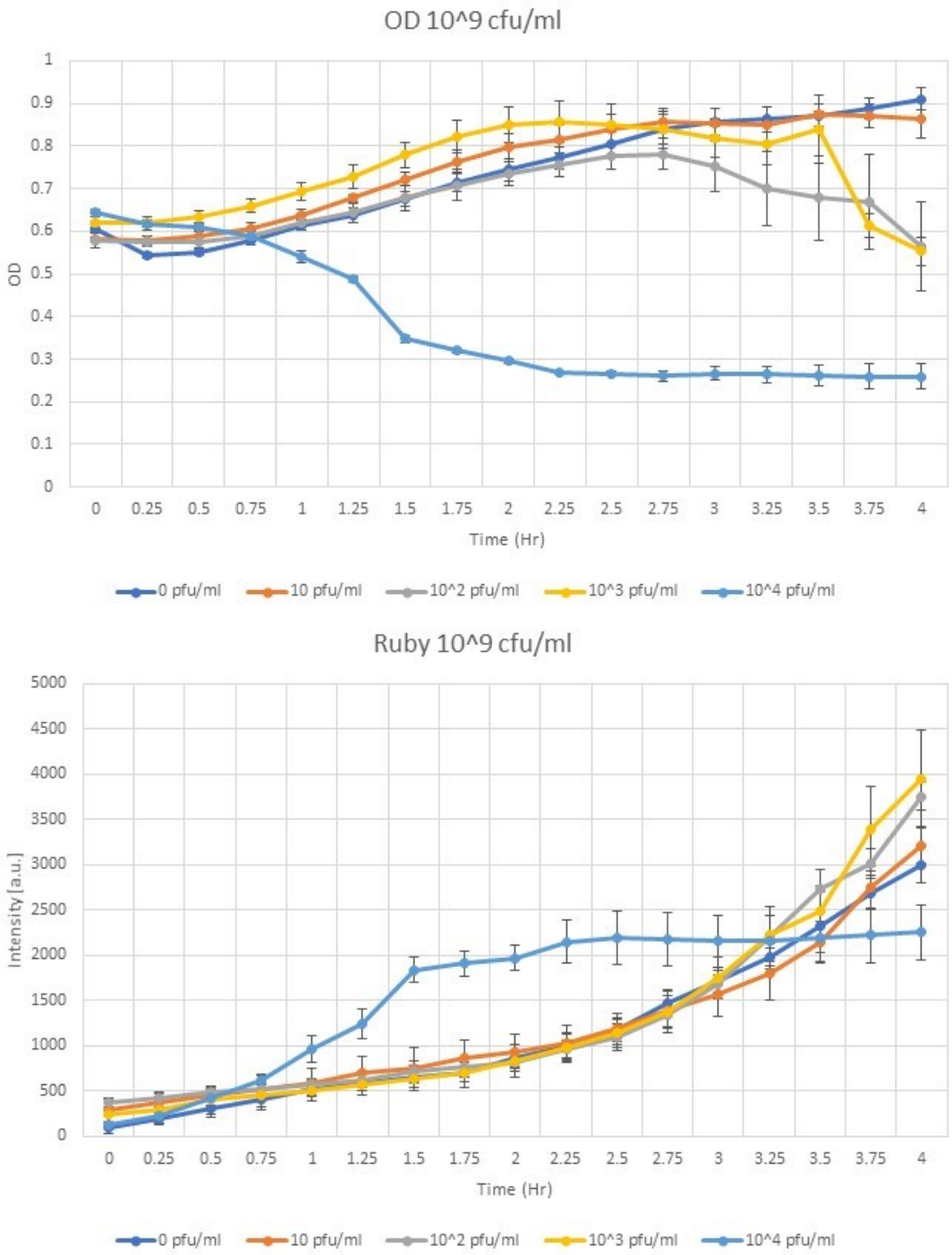

Figure 6: OD and ruby matrix emission intensity in phage treated bacteria. Data shown is average intensity across triplicates of a sample at the given condition. Increasing phage concentration increases the bacteria lysis rate.

Although the results in Figure 6 may appear to be different from those shown in Figure 5, it is important to note that the scale of the graphs is not the same, and the duration of the experiment was reduced from 16 hours to 4 hours. Repeating the experiments for 10^9 cfu/mL

yielded suprisingly different results than those seen in Figure 5. In terms of obvious similarities, it is seen that the 10^4 pfu/mL phage samples experience a significant decrease in OD and significant increase in ruby intensity at the 1-hour mark when compared with control. The 10^3 pfu/mL condition experiences significant decrease in OD and increase in Ruby intensity from control at the 3.75-hour mark. The 10^2 pfu/mL sees significant decrease in OD and increase in ruby intensity at the 4-hour mark.

These increasing-ruby-intensity and decreasing-OD time-points occur at slightly different times as compared to the initial 16-hour experiment. The 10^4 pfu/mL sample appears to experience a large increase in cell death around 1 hour prior to when it did in the 16-hour experiment, while all other phage conditions appear to experience the increase in cell death about 1 hour later than in the previous experiment. Regardless of this time difference, possibly due to consist pipetting error or to some issue with moving samples, the same overshoot of ruby intensity corresponding to significant decrease in OD is observed, however due to the time cutoff of data collection some of the other samples were not fully able to plateau in ruby intensity and OD. Although the experiment did not run as long as the original screening, it can be seen that for the 10^4 pfu/mL condition the end OD is near 0.2, similar to the original experiment. When compared to control, the lower phage concentrations show only a slight increase in ruby emission intensity at the same timepoint as when those samples also experience a larger decrease in OD. The 10^4 pfu/mL samples exhibit a plateauing behavior in both OD and ruby emission at the same times, after a significant overshoot in ruby signal as compared to control. This indicates that bacterial death is a large contributor to proteins being released into the EPS, as once the OD ceases to change, it is observed that ruby intensity does not change. Additionally, ruby intensity increases at a much higher rate for the 10^4 pfu/mL sample than others, during the same time at which the OD indicates higher death rate for that sample.

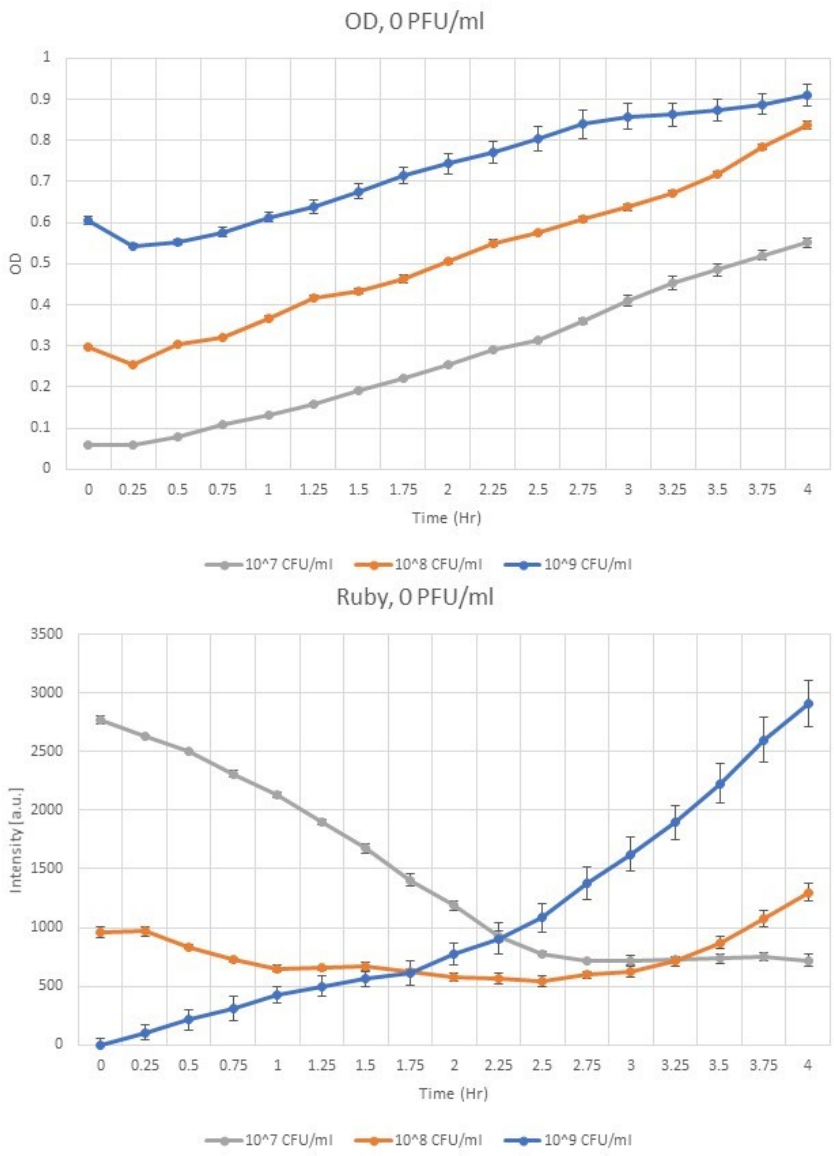

Figure 7: OD and ruby matrix emission intensity in control samples. As OD increases for all samples, only the higher bacterial concentration shows an increase in ruby emission, while the middle concentration showns almost no change in emission, and the lowest concentration shows an overall decrease.

Figure 7 reveals a key issue with ruby matrix that was not identified in an obvious and controlled manner up until this experiment. It appears that ruby matrix fluoresces at a much higher intensity when unbound as compared to when bound, behaving in a different manner to the intial stain screening experiment where these issues did not appear. In the intial screening experiments, it was observed that very little fluorescent signal was observed in control samples with no bacteria, where in this experiment, samples with bacteria in lower concentrations experience an abnormally high ruby signal. This raises the possibility that ruby matrix interacts with other EPS constituents, changing the fluorescent intensity of the stain when in the unbound state only.

However, if the ruby is at a low enough concentration relative to proteins in the EPS, as happens in the highest bacterial concentration used in some of the previous experiments, then most ruby matrix appears to have been bound to proteins in the EPS in some manner. This interpretation comes from comparing the results at different cfu (Figure 7). When examining the 10^7 cfu/mL sample OD and ruby intensities, it is observed that the final OD at the 4 hour point is slightly lower than the initial OD of the 10^9 cfu/mL sample, yet the ending ruby intensity of the lower concentration (10^7 cfu/mL) is still significantly higher than initial ruby intensity of the higher concentration. After considering the effects of possible photobleaching, a potential explanation is that higher amounts of dead bacteria contributed to the amount of protein in the EPS, allowing ruby to bind to proteins which are in a relatively higher amount when compared to higher bacterial concentrations. It is important to mention no normalization was carried out on any of the ruby intensities for Figures 5 through 7. Although this issue with unbound ruby exists, it should not impact the results discussed above for the 10^9 cfu/mL samples, as ruby behaves as expected at that high concentration where there is a sufficient amount of proteins to bind to.

DISCUSSION

The change in the environments contained within biofilms that undergo phage therapy is of importance when examining the efficacy of a therapy to both destroy bacteria and prevent regrowth or adaptation. Few studies have examined the changes that occur when biofilms are treated, only examining the causes that lead to destruction of a biofilm. Previous characterization involving pH has involved examining highly localized changes in pH and evaluating the use of pH probes in acquiring accurate readings within these structures.[9] pH has also been shown to be usable as an indicator of biofilm adaption in post antibiotic treatment scenarios in infected wastewater systems.[17] While understanding the relationship that pH has to viability of *P. aeruginosa* is outside the scope of this study, this work attempted to elucidate the changes that occur with phage therapy.

Interestingly, the results obtained from studying the control samples do not entirely agree with those obtained by Hunter *et al*.[9] It was expected that pH gradient as a function of depth in the biofilm would not change by much, which is the observation of this study. However, it was also expected that along the horizontal direction of the biofilm, the various microenvironments spanning only a few micrometers will vary within the pH range of 6.3 to 6.9. This study found that average pH's at various microenvironments were in the range of 5.6 to 5.8. This may possibly be attributed to difference in culture conditions in preparing the biofilms, the main difference being the use of flow cells to culture in an active flow environment, rather than a static environment. Culture times as well as seeding conditions were not significantly different from those used in previous studies utilizing CSNARF4.[9] With respect to phage treatment, it was shown that use of phages leads to a statistically significant but small decrease in the pH. Cell lysis and release of internal substances leads to more acidic conditions, antagonistic to the growth of bacteria.[11] Hunter *et al* has demonstrated that pH of 5.6 is the lower limit of biofilm survival, an acidic limit which was not seen in samples in this study. However, the biofilms that experienced death due to phage therapy were shown to be on the lower end of the pH range.[9] This contributes to the hypothesis that biofilm regrowth is stunted by pH changes as phages lyse bacterial cells. The inability to regrow allows phages to continuously act to destroy more bacteria in the biofilm. This insight, especially for this system, might be useful to take into account in an ongoing collaboration between the Curtis and Weitz groups, which are using computational modeling of phage-biofilm interactions to facilitate understanding and insights gathered from a large experimental data set. This proposed pH-dependent cell growth may likely apply to the WT NPAO1 strain of *P. aeruginosa*, as it was previously shown in *P. aeruginosa* biofilm samples retrieved from water waste systems, that bacterial regrowth after biofilm destruction is inhibited when biofilms are grown in conditions more acidic than near neutral pH's (i.e. 6.4 rather than 7.0).[11] At the same time, it is valuable to keep in mind that the process of biofilm-forming bacteria secreting various substances into the extracellular matrix may provide a natural buffering solution in which robust changes that are brought about by some treatments such as antibiotics are ineffective.[1,3,7,11]

One point of interest in relating the results of this study to the efficacy of phage treatment is examining the lowest area of biofilms, where it adheres to the surface and is most densely populated by bacteria. The pH for both untreated and phage-treated samples saw a dramatic increase in pH, leading to less acidic conditions at the depths of the biofilm. Although these pH's (5.8-5.9) are not far off in magnitude from the rest of the biofilm (5.6-5.7),they are closer to the pH range comfortable for bacterial growth. This suggests that bacterial death may be lower in the depths of the biofilm. Reduced death may be caused by phages not being able to access more dense parts of the biofilm or by buffering effects of other EPS components.

The limitations of utilizing a ratiometric probe to study pH *in vitro* are mainly a question of the chemical interactions that may come with the various extracellular polymeric substances existing within the biofilm matrix. Aggregation of the dye may also impact pH readings when using confocal microscopy to detect fluorescent intensities, although this was accounted for in this study through qualitative means, excluding areas with low signal in dense bacterial colonies. As previously discussed, aggregation within the cells for which dye may be able to permeate could impact the normal ways in which bacteria function. Other methods of examining pH in biofilms give only slightly worse resolution, such as microelectrode arrays, although they must be physically inserted thereby perturbing the biofilm physically. The use of a fluorescent dye, while it may permeate cells and effect the viability in that manner, is effectively the only way to study the impact that phages have on the pH of biofilms. Another limitation that was not considered in any possible phage interaction with the pH dye. A separate study would need to be done on the efficacy of phage therapy in the presence of this dye specifically to determine if the performance of the phage, either in terms of adsorption or mobility, is affected by this chemical. Even considering downsides of this, the ratiometric is useful if experiments are appropriately designed for imaging multiple targets apart from the pH probe itself. Another point is that the calibration of the dye, and the models used to evaluate emission intensity versus pH

The issue of ruby matrix not performing entirely as expected, fluorescing when unbound, does still give some insight into the process by which proteins specifically are released into the EPS matrix. The results gleaned otherwise by the data exhibited in this paper do not appear to be affected in a significant way by the unbound ruby matrix, due to the high concentrations of bacteria that were used to seed the cultures for the samples corresponding to the relevant data. This of course requires verification, if more time were available, processes for controlling unbound ruby would need to be explored before recompleting experiments. For phage treated samples, it appears that the dominant mechanism by which proteins are released into the EPS is not by bacteria spontaneously secreting proteins into the matrix as they form the biofilm structure, but is instead caused by the death of bacteria and subsequent release due to destruction of the cell barrier. Regardless, it was still displayed as expected that lysis of bacteria in the biofilm is a significant method by which proteins are released into the matrix of the biofilm, corresponding to the significant overshoot of ruby signal seen in the EPS experiments during increased bacterial death.

This issue of examining EPS in a static environment does bring up some limitations to the results found here. Prior studies, as discussed previously, used flow-cells to culture, treat, and image biofilms.[15,16] These flow cells used constant exposure and removal of the ruby stain, and would not encounter issues with unbound ruby remaining in samples. This constant flow environment would amount to avoiding the issue found in this study. Therefore, conditions for EPS examination in those studies may not be entirely applicable to what was found here when using a static growth-environment as compared to flow environments. Unsurprisingly the results due to the difference in the method of culturing may lead to entirely different conclusions if this was to be repeated using an active flow environment.[19,20] Remnant EPS was not expected nor controlled for in this study, although the results do not need to be voided for what was covered, as previously discussed. Thorough control testing when considering stain behavior in unbound scenarios should have been done prior to moving forward with the experiments utilizing stains, and in future, this needs to occur. Further improvements into the use of ruby matrix in static environment biofilm staining may also be necessary to avoid constant optimization of culture conditions.

CONCLUSION & FUTURE DIRECTIONS

This study examined the response of biofilms to phage treatment with respect to both changes in the pH gradient within the biofilm, as well as examining changes in EPS due to phage activity in biofilms. Maintaining a suitable internal pH in a biofilm is imperative in continuing growth and survivability of bacteria within the biofilms. It has been demonstrated that pH impacts *P. aeruginosa* viability in microenvironments in the biofilm, which is a potential area of study worth pursuing, especially with the combinatorial use of antibiotics and phages to eliminate more robust biofilms. Similar studies may also be of interest in the context of scenarios where biofilm destruction is crucial, such as dental biofilms, contaminants in wastewater, and infections on implanted medical devices. In dental biofilms for instance, it has been shown previously that pH's where bacteria remain viable to grow may reach extremely acidic conditions which are simultaneously harmful to the environment immediately external to the biofilm.[17] Changes in protein release contributing to the EPS in the biofilm matrix come about primarily due to increased cell death, while this does have an effect on buffering the pH environment, it also raises questions about the origin of other components of the EPS found in biofilms. Previous studies have indicated that other components of the biofilm matrix, such as polysaccharides, which are primarily secreted by cells, may be valid targets in terms of initiating biofilm destruction.[21] While targeting bacteria directly with phage treatment may be an effective strategy, it is still a possibility that increasing the densities of EPS in the matrix may have an adverse effect of further preventing destruction via bacteria-targeting agents. In the future, it may be of interest to study diffusion of phage into biofilms in both static and flow environments, to examine in depth whether destruction of bacteria has a significant shielding effect.

REFERENCES

1 Flemming, H.-C., & Wingender, J. (2010). The biofilm matrix. *Nature Reviews Microbiology*, *8*(9), 623–633. doi: 10.1038/nrmicro2415

2 Donlan, R. M. (2002). Biofilms: Microbial Life on Surfaces. *Emerging Infectious Diseases*, *8*(9), 881–890. doi: 10.3201/eid0809.020063

3 Reichhardt, C., Wong, C., Silva, D. P. D., Wozniak, D. J., & Parsek, M. R. (2018). CdrA Interactions within the Pseudomonas aeruginosa Biofilm Matrix Safeguard It from Proteolysis and Promote Cellular Packing. *MBio*, *9*(5). doi: 10.1128/mbio.01376-18

4 Sutherland, I. W., Hughes, K. A., Skillman, L. C., & Tait, K. (2004). The interaction of phage and biofilms. *FEMS Microbiology Letters*, *232*(1), 1–6. doi: 10.1016/s0378-1097(04)00041-2

5 Wu, Y.-K., Cheng, N.-C., & Cheng C.-M. (2019). Biofilms in Chronic Wounds: Pathogenesis and Diagnosis. *Trends in Biotechnology*, *37*(5), 505-517. doi:10.1016/j.tibtech.2018.10.011.

6 Lu, T. K., & Collins, J. J. (2007). Dispersing biofilms with engineered enzymatic bacteriophage. *Proceedings of the National Academy of Sciences*, *104*(27), 11197–11202. doi: 10.1073/pnas.0704624104

7 Shiley, J. R., Comfort, K. K., & Robinson, J. B. (2017). Immunogenicity and antimicrobial effectiveness of Pseudomonas aeruginosa specific bacteriophage in a human lung in vitro model. *Applied Microbiology and Biotechnology*, *101*(21), 7977–7985. doi: 10.1007/s00253-017-8504-1

8 Wolcott, R., Rhoads, D., Bennett, M., Wolcott, B., Costerton, J., Dowd, S. (2013). Chronic wounds and the medical biofilm paradigm. *Journal of Wound Care*, *19*(2). doi:10.12968/jowc.2010.19.2.46966.

9 Hunter, R. C., & Beveridge, T. J. (2005). Application of a pH-Sensitive Fluoroprobe (C-SNARF-4) for pH Microenvironment Analysis in Pseudomonas aeruginosa Biofilms. *Applied and Environmental Microbiology*, *71*(5), 2501–2510. doi: 10.1128/aem.71.5.2501-2510.2005

10 Burdíková, Z., Švindrych, Z., Pala, J., Hickey, C., Čmiel, V., Auty, M. A. E., & Sheehan, J. J. (2014). Fluorescence Lifetime pH Measurements in Cheese Matrix. *Microscopy and Microanalysis*, *20*(S3), 1358–1359. doi: 10.1017/s1431927614008526

11 Xiong, Y., Caillon, J., Drugeon, H., Potel, G., & Baron, D. (1996). Influence of PH on Adaptive Resistance of Pseudomonas Aeruginosa to Aminoglycosides and Their Postantibiotic

12 Erriu, M., Genta, G., Tuveri, E., Orrù, G., Barbato, G., & Levi, R. (2012). Microtiter spectrophotometric biofilm production assay analyzed with metrological methods and uncertainty evaluation. Measurement, 45(5), 1083-1088. doi:10.1016/j.measurement.2012.01.033

13 Schlafer, S., & Meyer, R. L. (2017). Confocal microscopy imaging of the biofilm matrix. *Journal of Microbiological Methods*, *138*, 50–59. doi: 10.1016/j.mimet.2016.03.002

14 Høiby, N., Ciofu, O., & Bjarnsholt, T. (2010). Pseudomonas aeruginosa biofilms in cystic fibrosis. *Future Microbiology*, *5*(11), 1663–1674. doi: 10.2217/fmb.10.125

15 Strathmann, M., Wingender, J., & Flemming, H.-C. (2002). Application of fluorescently labelled lectins for the visualization and biochemical characterization of polysaccharides in biofilms of Pseudomonas aeruginosa. *Journal of Microbiological Methods*, *50*(3), 237–248. doi: 10.1016/s0167-7012(02)00032-5

16 Ma, L., Conover, M., Lu, H., Parsek, M. R., Bayles, K., & Wozniak, D. J. (2009). Assembly and Development of the Pseudomonas aeruginosa Biofilm Matrix. *PLoS Pathogens*, *5*(3). doi: 10.1371/journal.ppat.1000354

Effects. *Antimicrobial Agents and Chemotherapy*, *40*(1), 35–39., doi:10.1128/aac.40.1.35.

17 Senneby, A., Davies, J., Svensater, G., & Neilands, J. (2017) Acid Tolerance Properties of Dental Biofilms in Vivo. *BMC Microbiology*, 17(1). doi:10.1186/s12866-017-1074-7.

18 Schlafer, S., Garcia, J. E., Greve, M., Raarup, M. K., Nyvad, B., & Dige, I. (2014). Ratiometric Imaging of Extracellular pH in Bacterial Biofilms with C-SNARF-4. *Applied and Environmental Microbiology*, *81*(4), 1267–1273. doi: 10.1128/aem.02831-14
19 Baird, F. J., Wadsworth, M. P., & Hill, J. E. (2012). Evaluation and optimization of multiple fluorophore analysis of a Pseudomonas aeruginosa biofilm. *Journal of Microbiological Methods*, *90*(3), 192-196. doi:10.1016/j.mimet.2012.05.004
20 Sanchez, Z., Tani, A., & Kimbara, K. (2012). Extensive Reduction of Cell Viability and Enhanced Matrix Production in Pseudomonas aeruginosa PAO1 Flow Biofilms Treated with a d-Amino Acid Mixture. *Applied and Environmental Microbiology*, *79*(4), 1396-1399. doi:10.1128/aem.02911-12
21 Ryder, C., Byrd, M., & Wozniak, D. J. (2007). Role of polysaccharides in Pseudomonas aeruginosa biofilm development. *Current Opinion in Microbiology*, *10*(6), 644-648. doi:10.1016/j.mib.2007.09.010